Determination of the distributions of degrees of acetylation of chitosan

Joel Jerushan Thevarajah, Matthew Paul van Leeuwen, Herve Cottet, Patrice Castignolles, Marianne Gaborieau

Determination of the Distributions of Degrees of Acetylation of Chitosan

Joel Jerushan Thevarajah[a,b], Matthew Paul Van Leeuwen[a,c], Herve Cottet[d], Patrice Castignolles[b*], Marianne Gaborieau[a,b]

[a] Western Sydney University, Molecular Medicine Research Group (MMRG), Parramatta campus, Locked bag 1797, Penrith 2751, Australia, joel.thevarajah@westernsydney.edu.au, m.gaborieau@westernsydney.edu.au

[b] Western Sydney University, Australian Centre for Research on Separation Sciences (ACROSS), School of Science and Health, Parramatta campus, Locked bag 1797, Penrith 2751, Australia, p.castignolles@westernsydney.edu.au

[c] Western Sydney University, School of Medicine, Parramatta campus, Locked bag 1797, Penrith 2751, Australia, m.vanleeuwen@westernsydney.edu.au

[d] Institut des Biomolécules Max Mousseron (IBMM, UMR 5247 CNRS-Université de Montpellier-Ecole Nationale Supérieure de Chimie de Montpellier), Place Eugène Bataillon CC 1706, 34095 Montpellier Cedex 5, France, herve.cottet@umontpellier.fr

* Corresponding author: p.castignolles@westernsydney.edu.au, tel: +61 2 9685 9970, fax: +61 2 9685 9915

Keywords: Chitosan; distribution of degrees of acetylation; capillary electrophoresis

Abstract

Chitosan is often characterized by its average degree of acetylation. To increase chitosan's use in various industries, a more thorough characterization is necessary as the acetylation of chitosan affects properties such as dissolution and mechanical properties of chitosan films. Despite the poor solubility of chitosan, free solution capillary electrophoresis (CE) allows a robust separation of chitosan by the degree of acetylation. The distribution of degrees of acetylation of various chitosan samples was characterized through their distributions of electrophoretic mobilities. These distributions can be obtained easily and with high precision. The heterogeneity of the chitosan chains in terms of acetylation was characterized through the dispersity of the

electrophoretic mobility distributions obtained. The relationship between the number-average degree of acetylation obtained by solid-state NMR spectroscopy and the weight-average electrophoretic mobilities was established. The distribution of degrees of acetylation was determined using capillary electrophoresis in the critical conditions (CE-CC).

1. Introduction

Chitosan is a polysaccharide derived from the *N*-deacetylation of chitin. Chitin is an abundant polysaccharide and it naturally occurs in the shells of arthropods such as shrimps, crabs and the cell walls of yeasts [1]. The molecular structure of the polysaccharide chitosan includes varying proportions of D-glucosamine and *N*-acetyl-D-glucosamine units (Fig. 1). Chitosan has several desirable properties that allowed it to become a significant area of research: it is biocompatible, biodegradable, antimicrobial and antifungal [2, 3]. In characterizing chitosan samples, a properly established structure-property relationship is required to assist in tailoring individual samples for specific uses [4, 5]. Therefore, accurately characterizing the supramolecular structure of chitosan is essential to understanding its properties. However, due to an incomplete understanding of chitosan's complex structure, several limitations exist in its characterization.

The degree of acetylation (*DA*) is defined as the fraction of *N*-acetyl-D-glucosamine units. The distributions of *DA*s correspond to the relative amount of chitosan macromolecules having a given *DA* plotted against *DA*. The existence of this distribution means that chitosan chains having different degrees of acetylation are present in a given sample. Although it has been well documented that a distribution of *DA*s exists (not all chitosan chains have the same *DA*), this is often overlooked [6, 7]. Due to its natural origin and the variation in processing conditions, chitosan can have broad distributions of *DA*s. The existence and importance of the distributions of the *DA*s has been revealed through a coupling of size-exclusion chromatography (SEC) separation with ^{1}H NMR spectroscopy detection; however, the distributions still have not been determined [6]. SEC [8], gradient SEC [9] and gradient liquid adsorption chromatography [10] have been used to determine chemical composition against molar mass (named "chemical composition distribution"), as well as distributions of composition in some cases [10, 11], for various copolymers, but not for chitosan. In addition, the distribution of compositions (or distribution of *DA*s for chitosan) have never been determined. The presence of a distribution of *DA*s can be attributed to the production of chitosan from chitin. Chitin exists in 3 forms, α, β and

γ [12]. The α and β forms vary in reactivity due to their structure. The α form is strongly stabilized by intra- and inter-sheet hydrogen bonds conversely to the β form which does not exhibit hydrogen bonding between successive chains. This results in β chitin being more soluble [13] as well as reactive [14]; however, the α form is more industrially available due to its natural abundance. Thus, heterogeneity is influenced by the structure of the chitin used in the production of chitosan.

The treatment of chitin to produce chitosan can also be a homogeneous or a heterogeneous process. The heterogeneous method has shown to be more effective in the deacetylation and is therefore more researched and used. A study in the heterogeneous deacetylation of both α and β chitin showed that in the deacetylation process two domains of deacetylation existed. There was also differences between α and β chitin which could be attributed to the structure of the α form preventing the accessibility of certain sites [15]. It was also identified that homogeneous deacetylation would increase the chance of a random distribution whereas heterogeneous deacetylation could cause blocks of acetylated/deacetylated units [16]. Block deacetylation is then attributed to the starting materials crystallinity in which the more amorphous region had the reactive acetylated sites more readily available and allowed a random distribution of acetylation [15].

Methods used to characterize chitosan by its average degree of acetylation/deacetylation previously include FTIR [17], Raman [18] and NMR spectroscopy [7, 19-21]. To determine the distribution of *DA*s, we require a method to identify the average degree of acetylation and a separation technique to identify the distribution of *DA*s. The most widely used method to separate polymers, especially polysaccharides, is size-exclusion chromatography (SEC) [22]. SEC separates polymers by their size (hydrodynamic volume) [23]. For chitosan this depends on both the molar mass and the degree of acetylation of the chitosan. Further, SEC analysis of chitosan has been plagued with aggregation [19]. Separation by composition is possible using liquid chromatography in the critical conditions [24] however, this can be extremely tedious and problematic [25] and is quasi-exclusively applied to organic system, and not aqueous system as used for chitosan. For this reason we propose to use free solution capillary electrophoresis (CE) for the analysis of chitosan by its degree of acetylation and its distributions [26, 27].

CE has been proven to effectively separate the polysaccharide pectin by composition. Several studies reported the separation of pectin by its degree of substitution (*DS*, which may include

esterification) [28]. Other research involved the use of capillary electrophoresis to determine the *DS* of caboxymethylcellulose [29]. Further, CE was proven to be a robust, reproducible method in the detection of impurities in the negatively charged biomolecule heparin [30]. The conditions of separation fall above the Manning condensation; however, separation is still possible although with a low selectivity. The separation of heparin is therefore very similar to that of chitosan. The ability to separate polymers by their composition independently from their molar mass is what differentiates CE from the aforementioned methods and makes it particularly appropriate for our study. It has been proven in the study of polylysine in which the electrophoretic mobility did not vary for a degree of polymerization above 4 [31]. This method is described as "in the critical conditions" (not referring to the separation mechanism but to the absence of separation by molar mass) and has been reviewed recently [26]. CE has previously been used in chitosan analysis including both native [7, 32] and modified chitosan [33].

To allow meaningful distributions to be obtained, the raw data, UV absorption against migration time, first needs to be converted into a distribution of electrophoretic mobilities, [34] and finally into chemical composition distributions. Different expressions of the dispersity of this distribution have recently been developed [27]. The dispersities determined from these different expressions are compared in this work in the case of chitosan. Analysis of the distributions of electrophoretic mobilities of cationic copolymers reveals information regarding their heterogeneity of composition. Understanding the heterogeneity of composition allows for property-structure relationships to be established. Expressions for the composition distributions were also established and tested for some block copolymers [27]. In this study, composition distributions for chitosan (under the form of distribution of *DA*s), or any statistical copolymer, are obtained for the first time.

2. Experimental section

2.1. Materials

Chitosan powders were purchased from Sigma-Aldrich, Castle Hill, Australia and from AK Biotech LTD, Jinan, China (Table S1). Samples were prepared at 1 $g \cdot L^{-1}$. Orthophosphoric acid (85 %) and boric acid were purchased from BDH AnalR, Merck Pty Ltd. Acetic acid (AcOH, glacial, 99 %) and hydrochloric acid (32 %) were purchased from Unilab. Poly(diallyldimethyl ammonium chloride) (PDADMAC 20 % in H_2O), alginic acid sodium salt, poly(allylamine

hydrochloride) (PAlAm), sodium hydroxide pellets, lithium hydroxide, sodium chloride, hexaamminecobalt(III) chloride (≥99.5 %), dimethyl sulfoxide (DMSO, ≥99.5 %) and adamantane (99 %) were purchased from Sigma-Aldrich. Sodium dihydrogen orthophosphate was purchased from Univar. Three ^{13}C singly labeled alanines were purchased from Cambridge isotope laboratories. All water used in this study was of Milli-Q quality. Sodium borate buffer (75 mM) was prepared from 0.5 M boric acid in Milli-Q water, titrated to pH 9.20 with 10 M sodium hydroxide, and diluted with Milli-Q water. Sodium phosphate buffer (100 mM) was prepared from 0.5 M sodium dihydrogen phosphate, titrated with phosphoric acid, and diluted with Milli-Q water. Lithium phosphate buffer (100 mM) was prepared from 85 % orthophosphoric acid, titrated to pH 2 with 10 M LiOH and diluted with Milli-Q water. Lithium phosphate, sodium borate and sodium phosphate buffers were sonicated for 5 min and filtered with a Millex GP polyethersulfone (PES) syringe filter (0.22 μm) before use.

2.2. Methods

2.2.1. Capillary Electrophoresis

Free solution capillary electrophoresis (CE) was carried out using an Agilent 7100 CE (Agilent Technologies, Waldbronn, Germany) instrument equipped with a diode array detector, contactless conductivity detector (TraceDeC, Innovative Sensor Technologies GmbH, Austria) and external circulating bath with MX temperature controller (Polyscience, USA). Polyimide-coated fused silica high sensitivity (HS) capillaries (50 μm internal diameter, bubble factor 3) were purchased from Agilent (Australia). Fused silica capillaries used for multilayer PDADMAC and alginate coatings with 50 μm internal diameter were purchased from Polymicro (USA)). The HS capillary (112.5 cm total length, 104 cm effective length) was initially pretreated by flushing for 10 min with 1 M NaOH, then 5 min with 0.1 M NaOH, Milli-Q water, and sodium borate, respectively at the start of a series of separations. The NaOH 1 M was prepared less than 24 h before use. In conditions of sodium borate (75 mM, pH 9.3) an oligoacrylate with a known separation [35] and a broad range of electrophoretic mobilities was injected to validate the capillary and the instrument before each session. After the standard separation and before the series of chitosan separations, the sodium borate was removed with a rinse method which included flushes for 5 min with 1M NaOH, 0.1M NaOH, and Milli-Q water, respectively, then a 10 min with 50 mM HCl and finally 5 min with either sodium or lithium phosphate. Before each

injection the capillary was rinsed with HCl (50 mM) and the background electrolyte (either sodium or lithium phosphate, 100 mM, pH 2) for 5 min each. Separation was obtained by applying 30 kV and 50 mbar pressure at 55 °C.

The fused silica capillary used for multilayer coatings was first treated for 45 min with 1 M NaOH and rinsed for 5 min with Milli-Q water. The coating process adapted from literature [36] included 45 min flushes with 2 % w/v PDADMAC in H_2O, then with 1 % w/v alginate in H_2O and finally 2 % w/v PDADMAC in H_2O. Following the coating process, the capillary was rinsed for 5 min with Milli-Q water and preconditioned before each injection for 10 min with 0.1 M NaOH and for 10 min with sodium phosphate (10 mM, pH 3). The separation was obtained by applying -30 kV at 25 °C.

The detection was set at 195 nm with a bandwidth of 10 nm.

2.2.2. Solid-State NMR spectroscopy

Solid-state ^{1}H and ^{13}C NMR spectra were recorded on a Bruker Avance DPX 200 spectrometer operating at Larmor frequencies of 200 MHz and 50 MHz, respectively. A commercial double resonance probe supporting zirconia MAS rotors with a 4 mm outer diameter and a 3 mm inner diameter was used, and samples were spun at 10 kHz at the magic angle. ^{1}H NMR spectra were recorded using a 5.73 µs 90° pulse, a 3 s repetition delay and at least 64 scans. ^{13}C CP-MAS NMR experiments were adapted from published quantitative measurements [19]. They were recorded with a 1 ms contact time and a 4 s repetition delay, and 21,586 to 104,924 scans. For ^{1}H experiments the 90° pulse was optimized using adamantane and power levels for the ^{13}C CP-MAS experiments were optimized using a mixture of three ^{13}C singly labeled alanines. The ^{1}H and ^{13}C chemical shifts scales were externally referenced using adamantane by setting the CH resonance to 1.64 and 38.48 ppm, respectively [37]. The degree of acetylation was measured through Eq. 1 [20]:

$$DA_n^{SSNMR}(\%) = \frac{I_{CH_3}}{(I_1+I_2+I_3+I_4+I_5+I_6)/6} \quad (1)$$

Where I_{CH3} is the integral of the methyl group of the acetyl group and I_1 to I_6 are the integrals of the signals assigned to the chitosan backbone.

3. Results and Discussions

3.1. Chitosan Dissolution

Analyzing a fully dissolved sample of chitosan in solution allows a complete characterization; however, obtaining a true solution of chitosan is quite difficult. In a previous study [19] the dissolution of chitosan was analyzed in a range of conditions with CE including the use of deuterated and aqueous solvents. Our new methodology to determine the distribution of electrophoretic mobilities and their dispersity [27] was applied to monitoring chitosan dissolution in aqueous solvent [19]. This allows further characterization of the dissolution. Initial CE separations of chitosan were based on apparent or electrophoretic mobility [7]. Pressure-assisted capillary electrophoresis (PACE) was used to analyze chitosan samples to obtain more precise electrophoretic mobility values [19]. This was necessary as deacetylation during the dissolution process is suspected and it could be detected only with sufficient precision in the measurement of electrophoretic mobility. PACE allowed the detection of both an internal standard and an electroosmotic flow marker (a neutral marker). It was noted previously that the weight-average electrophoretic mobility did not significantly vary with time of dissolution apart from the first 5 h in which incomplete dissolution led to high variations in electrophoretic mobility due to aggregation. In this work, the dispersity of the electrophoretic mobility distributions obtained were calculated and on the time scale exhibited similar behaviors for the different samples with the exception of LowMW1. MedMW samples were seen to have a similar dispersity over the period of dissolution with a slight increase in dispersity after the first 5 h suggesting that there was not a significant bias in dissolution (Fig. 2). The LowMW1 sample exhibited a very different dispersity with a large increase in dispersity after the initial 5 h. This suggests a bias in the dissolution with certain polymer chains with similar compositions dissolving first followed by the rest of the polymer chains. Therefore it is important to study the distributions of composition for chitosan as the *DA* may play a more important role than molar mass in the dissolution [27].

The kinetics of dissolution of MedMW in 50 mM HCl in H_2O was also compared to that in 50 mM DCl in D_2O (Fig. S1). No significant variation of dispersities of the $W(\mu)$ was observed. Following the dissolution study [19] 50 mM HCl at 60 °C for 2 hours was chosen in this work as the dissolution conditions for the range of commercially available chitosan samples with

different viscosities, degrees of acetylation (supplied and measured), molar masses and suppliers. This was to ensure minimal deacetylation during the dissolution.

3.2. Separation

3.2.1 Adsorption onto the capillary surface

It is important to optimize the conditions of separation to prevent unwanted broadening especially in the analysis of distributions. A factor that may negatively affect CE-CC separations is the adsorption of the polymer onto the surface of the capillary. To prevent adsorption a number of steps were taken including an increased cassette temperature and a lower pH buffer [19]. Multilayer coatings have been previously used to prevent the adsorption of proteins and plasma [36]. A cationic/anionic multilayer coating of PDADMAC and alginate was successfully tested with a model polyamine sample of poly(allylamine hydrochloride) (PAlAm). PAlAm was separated successfully (Fig. 3) in lithium phosphate 10 mM at pH 3 (LiPB10). A lower concentration of lithium phosphate buffer was used to prevent interaction with the multilayer coating. Detection of PAlAm was with UV at 195 nm as well as with a conductivity detector. The separation was also tested with sodium phosphate 10 mM at pH 3 (NaPB10); however, low sensitivity was experienced (Fig. S2). However, in the separation of chitosan with this coating, no chitosan peak was detected, assumingly because chitosan strongly adsorbs onto the coating, the signals detected at very high electrophoretic mobilities may correspond to either coating displaced by the chitosan or chitosan aggregates. It is assumed that chitosan has a higher affinity at pH 2 with alginate than PAlAm or PDADMAC. This prevented further use of the coating for chitosan characterization.

Although the multilayer coating was unable to be used to analyze chitosan, it has successfully been used in the separation of another cationic polymer. The methodology developed below could thus apply to a number of cationic polymers, even if they adsorbed onto standard fused silica capillaries.

3.2.2. Selectivity

To enhance the selectivity of the separation of chitosan in CE-CC compared to previous results [7, 19] various parameters were tested. This included the use of the surfactant Brij^{TM} 35 as a complexation reagent to adjust the selectivity [38]. However, chitosan did not dissolve in the

presence of Brij^{TM} 35 and remained as particulates. Brij^{TM} 35 also caused the precipitation of chitosan in solution, which prevented its analysis using CE (the use of an anionic surfactant would lead to water-insoluble complexes[39] and this was not attempted). Different counter-ions for the background electrolyte were also compared.

Chitosan was separated in sodium phosphate and lithium phosphate and the resulting electropherograms were analyzed (section 3.3). It was noted that chitosan was separated with a greater selectivity in lithium phosphate compared to sodium phosphate. The range of electrophoretic mobilities and dispersity values were determined as 3.0 to 4.8 (10^{-8} $m^2.V^{-1}.s^{-1}$) and 1.000 to 1.006 in sodium phosphate, as well as 2.7 to 4.8 (10^{-8} $m^2.V^{-1}.s^{-1}$) and 1.000 to 1.008 in lithium phosphate.

3.3 Electrophoretic mobility distributions

3.3.1 Chitosan in sodium phosphate

Appropriate treatment of the raw electropherograms [34] allowed meaningful mobility distributions to be obtained (Fig. 4A). The different chitosan samples were each seen to have a broad range of distributions of electrophoretic mobilities. The dispersity of the mobility distributions was calculated based on a ratio of moments [27] and plotted against the average *DA* measured by solid-state NMR spectroscopy (Fig. 4B). The dispersity was also plotted against the weight-average mobility (Fig. 4C). The general trend seen is that samples with a low average *DA* have a lower dispersity. This is expected as the heterogeneity of the composition is likely to increase as the *DA* increases (or decreases) until the composition becomes more homogeneous. The dispersity is seen to first increase and then decrease as the average *DA* increases. This trend is dissimilar to that which is seen for the dispersity against the weight-average electrophoretic mobility. As the weight-average electrophoretic mobility of the chitosan samples increases, their dispersity decreases.

3.3.2 Chitosan in lithium phosphate

In an effort to improve the selectivity of the chitosan separation, migration was also undertaken using LiPB100 as the background electrolyte (Fig. 5A). Lithium has a mobility (3.9 x 10^{-8} $m^2.V^{-1}.s^{-1}$) more similar to that of chitosan than sodium (5.2 x 10^{-8} $m^2.V^{-1}.s^{-1}$) [40]. This prevents the

occurrence of electrodispersion which may cause unwanted focusing and reduce selectivity further.

The distributions and dispersity values obtained of chitosan in LiPB100 showed similar trends to that in NaPB100. However, a greater repeatability was noted in the dispersity values of each of the samples.

Determining the dispersity of the electrophoretic mobility distributions is useful especially in the case of complex polyelectrolytes for which obtaining a correlation between the parameter of interest and mobility is challenging. Comparison of the dispersity values obtained from electrophoretic mobility distributions allows a direct qualitative comparison of the heterogeneity of the samples with respect to each other.

3.4. Composition distributions

3.4.1. Correlation between mobility and composition

To obtain composition distributions from electrophoretic mobility distributions a correlation is required between mobility and composition. Initial calibration curves which included all the chitosan samples used the average *DA* measured with solid-state NMR spectroscopy plotted against the weight-average electrophoretic mobility (Fig. S3). The *DA* values were measured using solid-state NMR spectroscopy as it was proven that analyzing the *DA* by solution-state NMR spectroscopy was inaccurate due to both poor dissolution or to deacetylation in the most commonly used solvents [19]. The initial calibration curves seemed to show 2 separate populations with a very low correlation. However, calibration curves, especially in the case of molar mass distributions, are generally made with narrow standards and the chitosan samples analyzed do not fit this criterion due to their heterogeneities of composition. Therefore to obtain a calibration curve samples were removed based on their dispersity value (below 1.0036 for LiPB100 ($r^2 > 0.75$) and 1.0040 for NaPB100 ($r^2 > 0.55$) until a correlation was obtained with a reasonable number of samples. This was undertaken for samples separated both in NaPB100 and Li-PB100. Using the least disperse samples for the calibration curve various fits including linear, polynomial, inverse and log functions were tested for the chitosan samples separated in NaPB100 (Fig. S4-7). All of the trends suffered from low correlation and the linear, inverse and log functions resulted in distributions containing populations with negative *DA* values. As the *DA* cannot physically fall below 0, the fit should rather be performed with a mathematical

function which is defined only between 0 and 1 (as is the *DA*). The Bradley function (double logarithmic reciprocal function) was thus tested and deemed the most appropriate fit (Equation 2 and Fig. 6).

$$\mu = a \times \ln\left(-b \times \ln(DA)\right) \quad (2)$$

Low correlations could be explained by a number of reasons. First the use of the Bradley fit is empirical (like that of the polynomial fit used for molar mass determination by SEC) but not based on a theory predicting the relation between μ and *DA*. Second, heterogeneity of the composition of chitosan is not just due to differences in average *DA* but may also be in the form of blocks of deacetylated groups. This would influence the separation as for the chitosan sample to be in the critical conditions for capillary electrophoresis the charges should be evenly distributed along the polymer chain. If there are blocks of charged species the chitosan chains may behave as a block copolymer [41] rather than a statistical copolymer. In this case the separation (electrophoretic mobility) is influenced by both the mobility of the charged species and the hydrodynamic friction of the uncharged species. Without an appropriate correction factor the occurrence of this bias cannot be accounted for. One reason for block deacetylation is the semi-crystalline structure of the precursor of chitosan, chitin [42]. To check if the occurrence of 2 populations was due to block deacetylation XRD measurements were undertaken. Crystallinity from the precursor chitin would likely play a role in the block deacetylation. However no significant difference was noted between the samples which exhibited diffractograms typical of amorphous chitosan samples [43] (Fig. S8). This suggests that no long range order is in the chitosan samples; however, the occurrence of short chain blocks is still possible and would influence the mobility. Further reasons of a low correlation may include the dissolution and the treatment of chitin to chitosan. The dissolution of the sample plays an important role in the meaningful characterization of the sample as a whole and bias in dissolution would prevent an accurate correlation between the accurate *DA* measured in solid-state NMR spectroscopy and the distributions of mobility. Although the problem of dissolution was not overcome and requires further investigation, composition distributions were obtained with the best current dissolution.

3.4.2. Calculation of composition distributions

Using the calibration curve the electrophoretic mobility distributions were transformed to composition distributions using the following equations:

$$DA = exp\left(-\frac{exp\left(\frac{\mu}{a}\right)}{b}\right) (3)$$

$$W(DA) = W(\mu) \times \frac{-a}{DA \times \ln(DA)} (4)$$

The composition distributions of the chitosan samples used in calibration curves were obtained (Fig. 7). This is the first time composition distributions of chitosan are presented in the literature. The composition distributions reveal information on the amount of chains with a specific composition in the sample. The dispersities of the composition distributions were observed to be larger than those seen for electrophoretic mobility distributions (Fig. 8). There is no expectation of the dispersities values for these two different types of distributions to be similar. However, larger variations in dispersity values of the composition distributions were seen between replicates. The dispersity values of the composition distributions are less repeatable than the ones of the electrophoretic mobility distributions; however, the variations were still small (e.g. in comparison to the 2000 % variation for M_n and M_w determined in a round-robin test for poly(acrylic acid) using SEC [44]). The dispersity values were calculated for composition distributions for the first time. The dispersity values for $D(W(\mu),1,0)$ were determined to be larger than those for $D(W(\mu),2,0)$ and $D(W(\mu),3,0)$. A different trend of the dispersity values was seen compared to those calculated from the electrophoretic mobility distributions. This is likely due to the lower selectivity in terms of μ at low *DA* compared to intermediate *DA* (the calibration curve has a higher slope at low *DA* than intermediate *DA*). The conversion from $W(\mu)$ to $W(DA)$ thus corrects an artefact in a similar fashion as the conversion from SEC chromatograms to molar mass distributions corrects for an artefact when the SEC calibration is not linear in the region of interest [45]. Standard deviation values of $W(DA)$ showed a trend similar to that obtained with the dispersities of $W(\mu)$. The dispersity of $W(DA)$ and its standard deviation thus give different information on the composition and its heterogeneity. They may relate to different functional properties. The standard deviation values are corresponding to the visual comparison of the $W(DA)$: the distributions at the lowest *DA*s appear sharper. It is to note that the translation of the $W(DA)$ at higher *DA* (+0.05) led to a decrease of the dispersity values from around 2 (Fig. 7) to 1.0001. The dispersity values are thus giving an interesting perspective on the $W(DA)$ that visual observation of the distributions in this work could not provide. Properties (such as some

mechanical properties) affected by both the magnitude of *DA* and the width of the distribution of *DA*s might relate to $D(W(DA),1,0)$, $D(W(DA),2,0)$ or $D(W(DA),3,0)$. Properties affected primarily by the width of the distribution of *DA*s, rather than the magnitude of *DA* (such as adhesive vs cohesive failure in adhesives) might relate to standard deviation.

Using the composition distributions obtained (Fig. 7B) a second iteration of the *DA* versus electrophoretic mobility calibration curve was determined for the chitosan samples separated in LiPB100. There is no reason for the average *DA* determined by NMR to correspond to μ_w. To obtain the second iteration the average *DA* values determined from the solid-state NMR measurements were thus replaced with those determined at the peak apex of the relevant composition distributions. This was re-plotted against the weight-average electrophoretic mobilities obtained by CE (Fig. 6B). The correlation improved compared to the initial calibration curve. This was not the case for the chitosan samples separated in NaPB100 (Fig. S9). Therefore, composition distributions were calculated for the chitosan samples using the 2nd iteration of the calibration curve only in LiPB100. Further the dispersity values of the composition distributions were plotted against the *DA* obtained by solid-state NMR spectroscopy (Fig. 9B). The composition distributions exhibited minimal changes, although slightly more tailing may be noticed. The trend of the dispersity values is similar to that before the iteration. Once again the standard deviation supports the visual observation for the composition distributions; however, the corresponding values are higher in the re-treated composition distributions. The dispersity values are constant throughout the whole range of samples. Therefore a quantitative analysis of the composition distributions is possible using the standard deviation which discriminates the different chitosan in this work and potentially the dispersities for other samples.

4. Conclusions

In this study distributions of electrophoretic mobilities and of compositions were obtained for a range of chitosan samples and their dispersity values were determined. Multilayer coatings were tested to prevent adsorption and a cationic polymer, polyamine sample poly(allylamine hydrochloride) was separated successfully. The selectivity of the chitosan separation was improved with the use of lithium as the counter-ion. The distribution of electrophoretic mobilities, $W(\mu)$, and its dispersity can be used for a quick and precise characterization of the

heterogeneity of *DA* of chitosan (or the heterogeneity of composition of any statistical copolymer where at least one monomer unit is charged). The application of this methodology to the monitoring of the dissolution of chitosan confirmed that the *DA* can influence the dissolution of chitosan. Strategies to obtain the distribution of *DAs*, *W*(*DA*), have been proposed and tested as well. The determination of *W*(*DA*) requires establishing a correlation between the *DA* of several chitosan samples and their electrophoretic mobility. The usual mathematical functions (linear, polynomial) used to produce calibration curves (in SEC) did not provide any correlation. Bradley functions did provide some correlation between the weight-average electrophoretic mobility and the *DA* (composition) of chitosan samples which allowed composition distributions to be obtained for the first time. Standard with low dispersity of the distribution of *DA*s do not exist. The quality of the calibration can thus be rather improved by using an iteration process (in which the peak apex from the composition distributions is used as an improved *DA* value). For the specific example of chitosan, the standard deviation and dispersity were valuable in numerically representing the heterogeneity of the composition distributions and give different perspectives. This methodology can be applied to any charged copolymer such as heparin, carboxymethylcelluloses and pectins and would truly be advantageous. Separations by composition with a high selectivity would allow a strong correlation between mobility and composition. Further work may also involve improving the selectivity specifically in the separation of chitosan. This would result in a greater precision and potentially great accuracy in the resulting composition distributions. In conclusion, the calculation of composition distributions provides an improved characterization which influences the possible modification or functionalization of copolymers, quality control of the synthesis and a closer step towards understanding structure-property relationships of complex polymers, which has already been identified as crucial. For example the *DA* has been shown to influence significant properties such as bioadhesion [5], dissolution [19] and biodegradability [46, 47]. The functional characterization of chitosan and its derivatives is nowadays one of the most productive research areas [3].

Supporting Information

The supporting information contains the supplier information, kinetics of dissolution, separation of PAlAm, correlation of electrophoretic mobility and composition and X-ray diffraction of chitosan powders.

Acknowledgments

JJT thanks Leena Thevarajah for assistance with data treatment, Aidan Grosas for discussions, Alison Maniego and Melissa Meinel for assistance in the lab. JJT also thanks the Australian Government for an Endeavour Research fellowship to travel to the University of Montpellier, Montpellier, France. The authors thank Timothy Murphy and Richard Wuhrer from the Advanced Materials Characterisation Facility (AMCF) at Western Sydney University for discussions and instrumentation training/assistance.

References

[1] M. Rinaudo, Chitin and chitosan: Properties and applications, Prog. Polym. Sci. 31 (2006) 603-632.

[2] A. Domard, A perspective on 30 years research on chitin and chitosan, Carbohydr. Polym. 84 (2011) 696-703.

[3] S.K. Shukla, A.K. Mishra, O.A. Arotiba, B.B. Mamba, Chitosan-based nanomaterials: A state-of-the-art review, Int. J. Biol. Macromol. 59 (2013) 46-58.

[4] M.J. Barton, J.W. Morley, D.A. Mahns, D. Mawad, R. Wuhrer, D. Fania, S.J. Frost, C. Loebbe, A. Lauto, Tissue repair strength using chitosan adhesives with different physical-chemical characteristics, J. Biophotonics 7 (2014) 948-955.

[5] B. Menchicchi, J.P. Fuenzalida, K.B. Bobbili, A. Hensel, M.J. Swamy, F.M. Goycoolea, Structure of Chitosan Determines Its Interactions with Mucin, Biomacromolecules 15 (2014) 3550-3558.

[6] S. Nguyen, S. Hisiger, M. Jolicoeur, F.M. Winnik, M.D. Buschmann, Fractionation and characterization of chitosan by analytical SEC and H-1 NMR after semi-preparative SEC, Carbohydr. Polym. 75 (2009) 636-645.

[7] M. Mnatsakanyan, J.J. Thevarajah, R.S. Roi, A. Lauto, M. Gaborieau, P. Castignolles, Separation of chitosan by degree of acetylation using simple free solution capillary electrophoresis, Anal. Bioanal. Chem. 405 (2013) 6873-6877.

[8] I.A.H. Ahmad, A.M. Striegel, Determining the absolute, chemical-heterogeneity-corrected molar mass averages, distribution, and solution conformation of random copolymers, Anal. Bioanal. Chem. 396 (2010) 1589-1598.

[9] H. Maier, F. Malz, W. Radke, Characterization of the Chemical Composition Distribution of Poly(n-butyl acrylate-stat-acrylic acid)s, Macromol. Chem. Phys. 216 (2015) 228-234.

[10] M. Shakun, T. Heinze, W. Radke, Determination of the DS distribution of non-degraded sodium carboxymethyl cellulose by gradient chromatography, Carbohydr. Polym. 98 (2013) 943-950.

[11] M. Shakun, T. Heinze, W. Radke, Characterization of sodium carboxymethyl cellulose by comprehensive two-dimensional liquid chromatography, Carbohydr. Polym. 130 (2015) 77-86.

[12] M.K. Jang, B.G. Kong, Y.I. Jeong, C.H. Lee, J.W. Nah, Physicochemical characterization of alpha-chitin, beta-chitin, and gamma-chitin separated from natural resources, J. Polym. Sci. Pol. Chem. 42 (2004) 3423-3432.

[13] T. Sannan, K. Kurita, Y. Iwakura, Studies on Chitin, 2. Effect of Deactylation on Solubility, Makromol. Chem. Macromol. Chem. Phys. 177 (1976) 3589-3600.

[14] K. Kurita, S. Ishii, K. Tomita, S.I. Nishimura, K. Shimoda, Reactivity Characteristics of Squid Beta-Chitin as Compared with Those of Shrimp Chitin: High Potentials of Squid Chitin as

a Starting Material for Facile Chemical Modifications, J. Polym. Sci. A Polym. Chem. 32 (1994) 1027-1032.

[15] G. Lamarque, C. Viton, A. Domard, Comparative study of the first heterogeneous deacetylation of alpha- and beta-chitins in a multistep process, Biomacromolecules 5 (2004) 992-1001.

[16] K. Kurita, T. Sannan, Y. Iwakura, Studies on Chitin, 4. Evidence for formation of block and random copolymers of N-Acetyl-D-glucosamine and D-glucosamine by Hetero- and Homogenous Hydrolyses, Macromol. Chem. Phys. 178 (1977) 3197-3202.

[17] M.R. Kasaai, Various Methods for Determination of the Degree of N-Acetylation of Chitin and Chitosan: A Review, J. Agric. Food Chem. 57 (2009) 1667-1676.

[18] A. Zajac, J. Hanuza, M. Wandas, L. Dyminska, Determination of N-acetylation degree in chitosan using Raman spectroscopy, Spectroc. Acta Pt. A-Molec. Biomolec. Spectr. 134 (2015) 114-120.

[19] J.J. Thevarajah, J.C. Bulanadi, M. Wagner, M. Gaborieau, P. Castignolles, Towards a less biased dissolution of chitosan, Anal. Chim. Acta 935 (2016) 258-268.

[20] M.H. Ottoy, K.M. Varum, O. Smidsrod, Compositional heterogeneity of heterogeneously deacetylated chitosans, Carbohydr. Polym. 29 (1996) 17-24.

[21] L. Heux, J. Brugnerotto, J. Desbrieres, M.F. Versali, M. Rinaudo, Solid state NMR for determination of degree of acetylation of chitin and chitosan, Biomacromolecules 1 (2000) 746-751.

[22] M. Gaborieau, P. Castignolles, Size-exclusion chromatography (SEC) of branched polymers and polysaccharides, Anal. Bioanal. Chem. 399 (2011) 1413-1423.

[23] Z. Grubisic, P. Rempp, H. Benoit, A universal calibration for gel permeation chromatography (Reprinted from Polymer Letters, vol 5, pg 753-759, 1967), J. Polym. Sci. B Polym. Phys. 34 (1996) 1707-1713.

[24] Y. Brun, P. Foster, Characterization of synthetic copolymers by interaction polymer chromatography: Separation by microstructure, J. Sep. Sci. 33 (2010) 3501-3510.

[25] A. Favier, C. Petit, E. Beaudoin, D. Bertin, Liquid chromatography at the critical adsorption point (LC-CAP) of high molecular weight polystyrene: pushing back the limits of reduced sample recovery, E-Polymers 9 (2009) 15.

[26] J.J. Thevarajah, M. Gaborieau, P. Castignolles, Separation and characterization of synthetic polyelectrolytes and polysaccharides with capillary electrophoresis, Adv. Chem. 2014 (2014) Article ID 798403.

[27] J.J. Thevarajah, A.T. Sutton, A.R. Maniego, E.G. Whitty, S. Harrisson, H. Cottet, P. Castignolles, M. Gaborieau, Quantifying the Heterogeneity of Chemical Structures in Complex Charged Polymers through the Dispersity of Their Distributions of Electrophoretic Mobilities or of Compositions, Anal. Chem. 88 (2016) 1674-1681.

[28] S.E. Guillotin, E.J. Bakx, P. Boulenguer, H.A. Schols, A.G.J. Voragen, Determination of the degree of substitution, degree of amidation and degree of blockiness of commercial pectins by using capillary electrophoresis, Food Hydrocoll. 21 (2007) 444-451.

[29] K.A. Oudhoff, F.A. Ab Buijtenhuijs, P.H. Wijnen, P.J. Schoenmakers, W.T. Kok, Determination of the degree of substitution and its distribution of carboxymethylcelluloses by capillary zone electrophoresis, Carbohydr. Res. 339 (2004) 1917-1924.

[30] T. Wielgos, K. Havel, N. Ivanova, R. Weinberger, Determination of impurities in heparin by capillary electrophoresis using high molarity phosphate buffers, J. Pharm. Biomed. Anal. 49 (2009) 319-326.

[31] H.F. Wu, S.A. Allison, C. Perrin, H. Cottet, Modeling the electrophoresis of highly charged peptides: Application to oligolysines, J. Sep. Sci. 35 (2012) 556-562.

[32] C.H. Wu, C.Y. Kao, S.Y. Tseng, K.C. Chen, S.F. Chen, Determination of the degree of deacetylation of chitosan by capillary zone electrophoresis, Carbohydr. Polym. 111 (2014) 236-244.

[33] C. Lefay, Y. Guillaneuf, G. Moreira, J.J. Thevarajah, P. Castignolles, F. Ziarelli, E. Bloch, M. Major, L. Charles, M. Gaborieau, D. Bertin, D. Gigmes, Heterogeneous modification of chitosan via nitroxide-mediated polymerization, Polym. Chem. 4 (2013) 322-328.

[34] J. Chamieh, M. Martin, H. Cottet, Quantitative Analysis in Capillary Electrophoresis: Transformation of Raw Electropherograms into Continuous Distributions, Anal. Chem. 87 (2015) 1050-1057.

[35] M. Gaborieau, T. Causon, Y. Guillaneuf, E.F. Hilder, P. Castignolles, Molecular weight and tacticty of oligoacrylates by capillary electrophoresis - mass spectrometry, Aus. J. Chem. 63 (2010) 1219-1226.

[36] H. Katayama, Y. Ishihama, N. Asakawa, Stable cationic capillary coating with successive multiple ionic polymer layers for capillary electrophoresis, Anal. Chem. 70 (1998) 5272-5277.

[37] C.R. Morcombe, K.W. Zilm, Chemical shift referencing in MAS solid state NMR, J. Magn. Reson. 162 (2003) 479-486.

[38] M.T. Bowser, E.D. Sternberg, D.D.Y. Chen, Development and application of a nonaqueous capillary electrophoresis system for the analysis of porphyrins and their oligomers, Anal. Biochem. 241 (1996) 143-150.

[39] L. Chiappisi, M. Gradzielski, Co-assembly in chitosan-surfactant mixtures: thermodynamics, structures, interfacial properties and applications, Adv. Colloid Interface Sci. 220 (2015) 92-107.

[40] J. Wu, K. Gerstandt, H. Zhang, J. Liu, B.J. Hinds, Electrophoretically induced aqueous flow through single-walled carbon nanotube membranes, Nat. Nano. 7 (2012) 133-139.

[41] A.T. Sutton, E. Read, A.R. Maniego, J. Thevarajah, J.D. Marty, M. Destarac, M. Gaborieau, P. Castignolles, Purity of double hydrophilic block copolymers revealed by capillary electrophoresis in the critical conditions, J. Chromatogr. A 1372 (2014) 187-195.

[42] C.K.S. Pillai, W. Paul, C.P. Sharma, Chitin and chitosan polymers: Chemistry, solubility and fiber formation, Prog. Polym. Sci. 34 (2009) 641-678.

[43] C. Gartner, B.L. Lopez, L. Sierra, R. Graf, H.W. Spiess, M. Gaborieau, Interplay between Structure and Dynamics in Chitosan Films Investigated with Solid-State NMR, Dynamic Mechanical Analysis, and X-ray Diffraction, Biomacromolecules 12 (2011) 1380-1386.

[44] D. Berek, Size exclusion chromatography - A blessing and a curse of science and technology of synthetic polymers, J. Sep. Sci. 33 (2010) 315-335.

[45] M. Gaborieau, R.G. Gilbert, A. Gray-Weale, J.M. Hernandez, P. Castignolles, Theory of Size Exclusion Chromatography (SEC) of complex branched polymers, Macromol. Theory Simul. 16 (2007) 13-28.

[46] Y. Shigemasa, K. Saito, H. Sashiwa, H. Saimoto, Enzymatic Degradation of Chitins and Partially Deacetylated Chitins, Int. J. Biol. Macromol. 16 (1994) 43-49.

[47] S. Aiba, Studies on Chitosan 4. Lysozyme Hydrolysis of Partially N-Acetylated Chitosans, Int. J. Biol. Macromol. 14 (1992) 225-228.

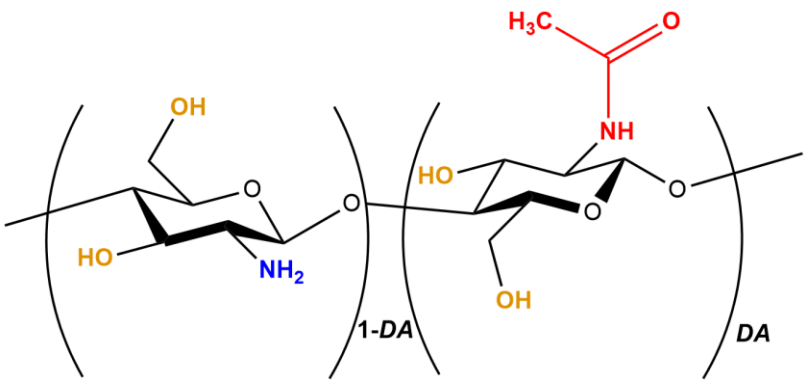

Figure 1. Chemical structure of chitosan (of degree of acetylation *DA*) and of chitin (for *DA*=1).

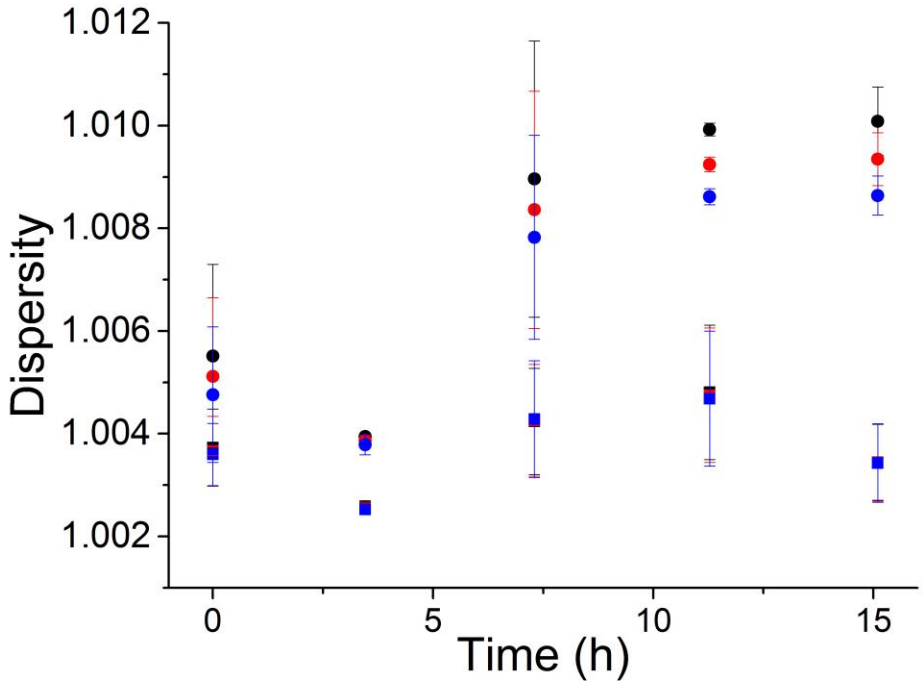

Figure 2. Dispersity $D(W(\mu),1,0)$ (black), $D(W(\mu),2,0)$ (red) and $D(W(\mu),3,0)$ (blue) of chitosan MedMW1 (squares) and LowMW1 (circles) during kinetic measurement of dissolution in 50 mM HCl in H_2O using CE-CC with the carousel kept at 60 °C. See supporting information equation S1 to S3 for dispersity calculations [27].

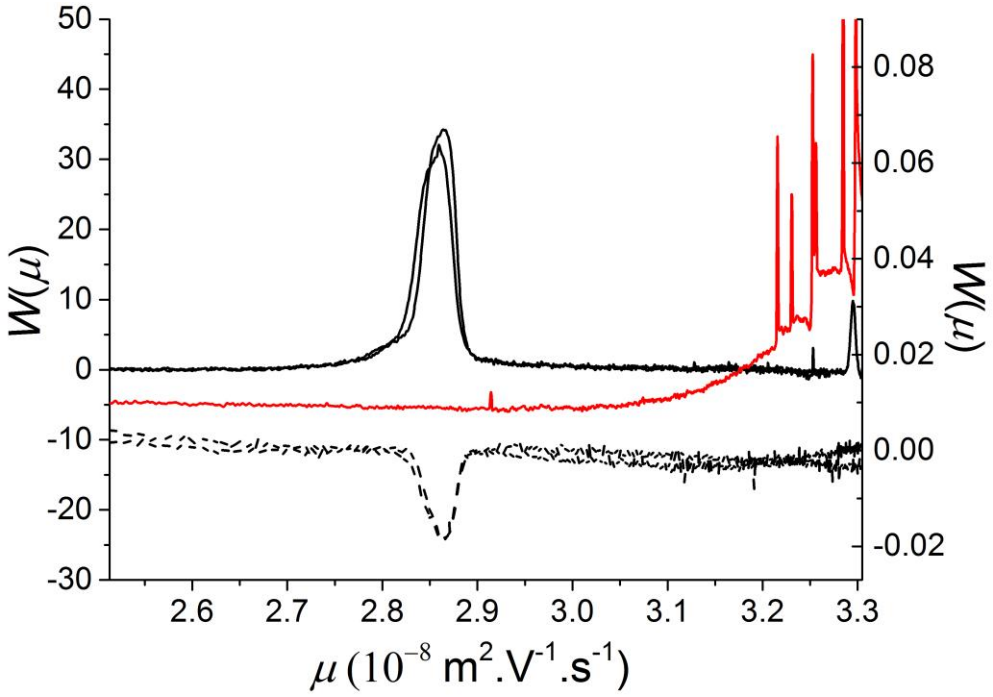

Figure 3. Electropherogram of PAlAm (black lines) and chitosan (red line) separated in a PDADMAC/alginate/PDADMAC coated capillary (50 cm total length) in LiPB10 at -30 kV with UV (solid line – left y axis) and contactless capacitively-coupled conductivity (dashed line – right y axis) detections. Where μ is the electrophoretic mobility and $W(\mu)$ is the weight fraction of polyelectrolyte chains with a given electrophoretic mobility calculated as the absorbance ($S(t)$) multiplied by the migration time.

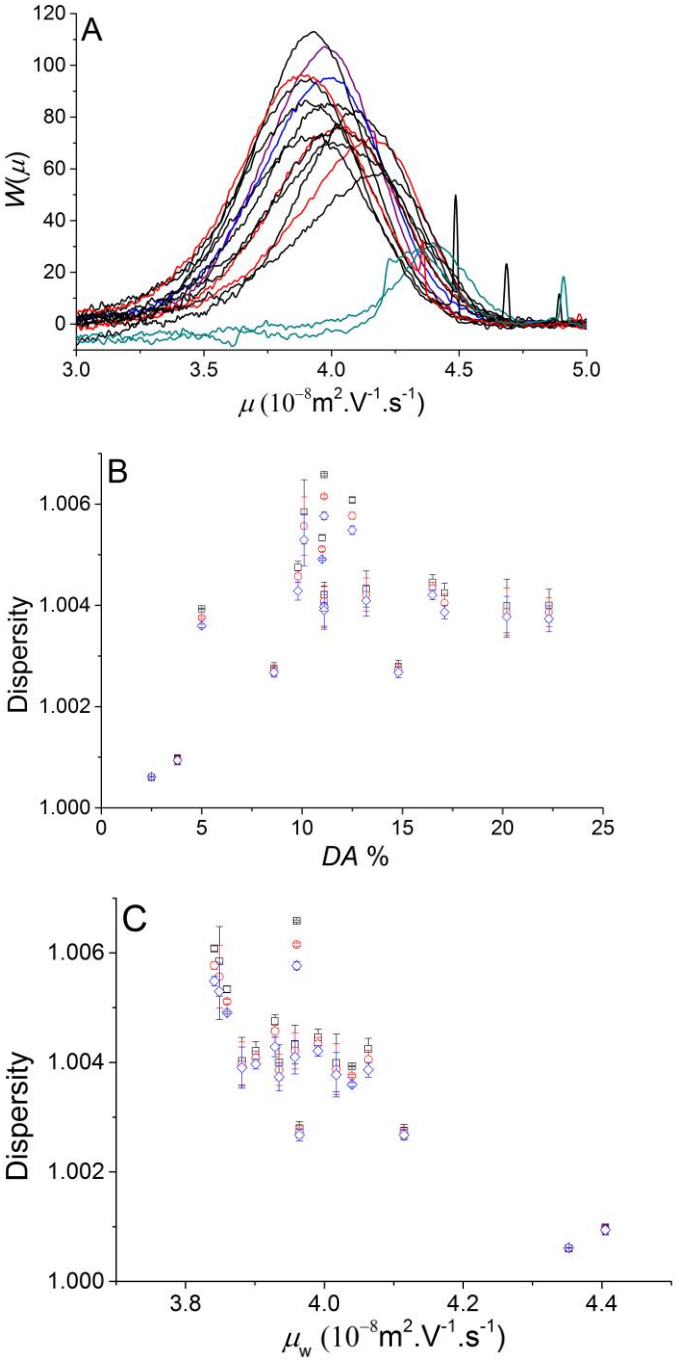

Figure 4. A. Distribution of electrophoretic mobilities, $W(\mu)$, of chitosan separated with PACE using NaPB100 for samples with an average *DA* (measured by SSNMR) below 5 % (green lines), between 5 % and 10 % (blue line), between 10 % and 15 % (red lines), between 15 % and 20 % (black lines) and above 20 % (purple line). Dispersity values (see supporting information for expressions) for chitosan samples as $D(W(\mu),1,0)$ (black squares), $D(W(\mu),2,0)$ (red circles) and $D(W(\mu),3,0)$ (blue diamonds) against their (B) number-average degree of acetylation or (C) weight-average electrophoretic mobility (μ_w). See supporting information equation S1 to S3 for dispersity calculations [27].

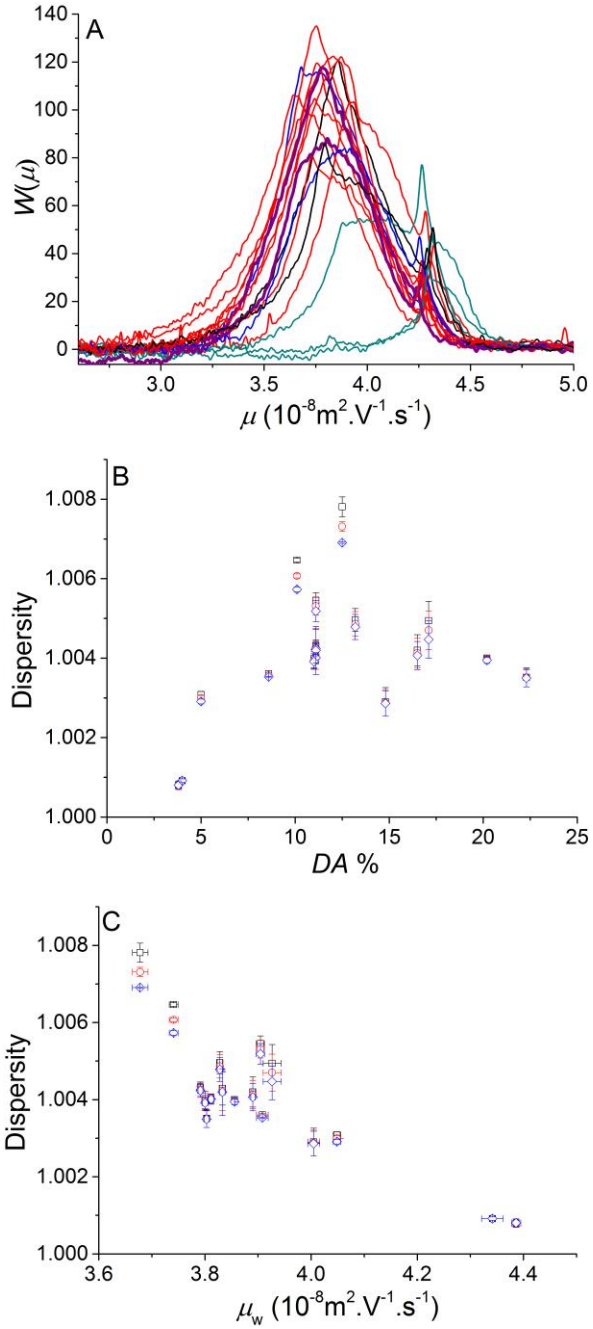

Figure 5. A. Distributions of electrophoretic mobilities, *W(μ)*, of chitosan separated with PACE using LiPB100 with samples with an average *DA* below 5 % (green lines), between 5 % and 10 % (blue line), between 10 % and 15 % (red lines), between 15 % and 20 % (black lines) and above 20 % (purple line). Dispersity values for chitosan samples as *D*(*W*(*μ*),1,0) (black squares), *D*(*W*(*μ*),2,0) (red circles) and *D*(*W*(*μ*),3,0) (blue diamonds) against their (B) number-average degree of acetylation or (C) weight-average electrophoretic mobility. See supporting information equation S1 to S3 for dispersity calculations [27].

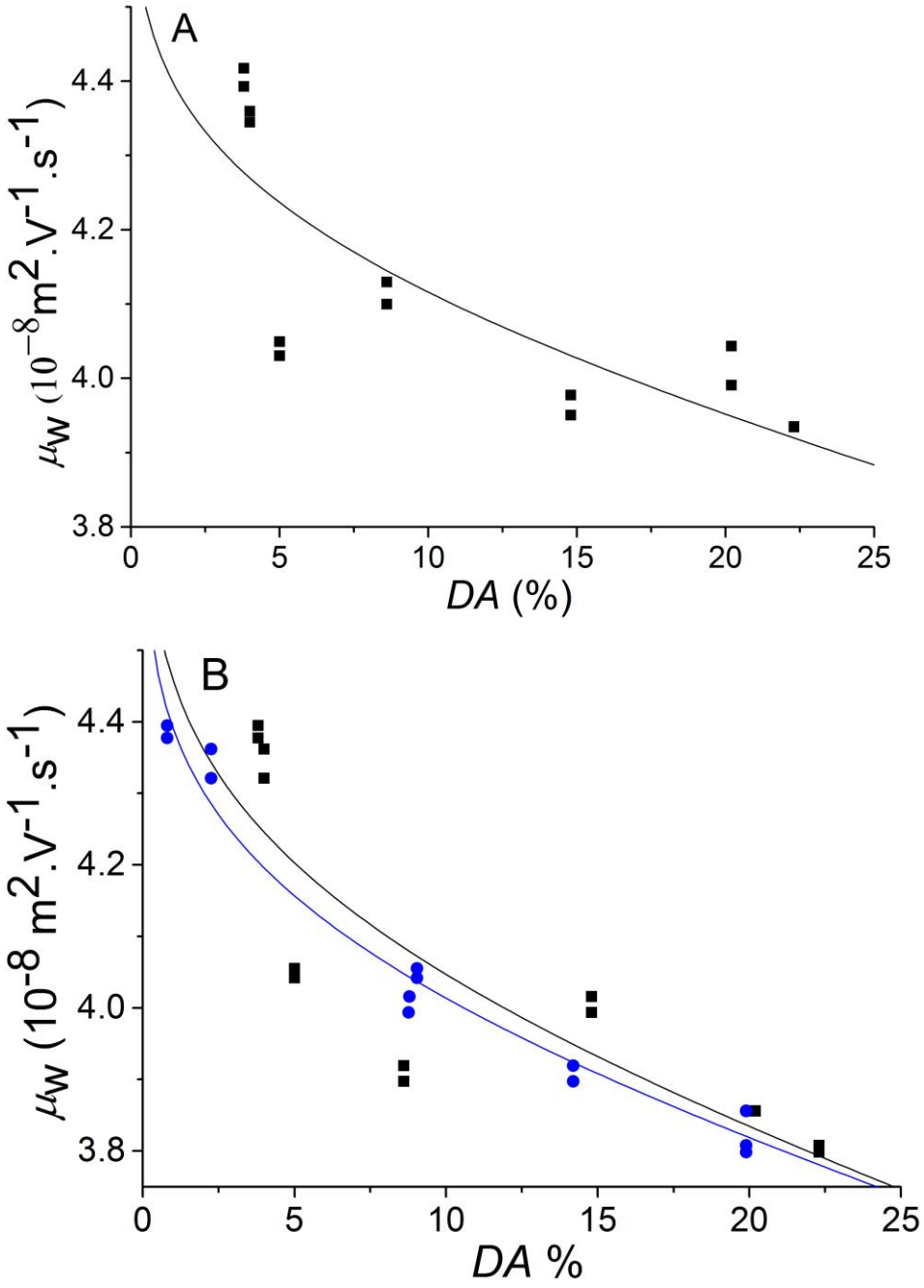

Figure 6. Calibration curve of the weight-average electrophoretic mobility in A. NaPB100 (a = 4.58×10^{-9}, b = 3447.2, $r^2 = 0.62$) B. LiPB100 as a function of *DA* for chitosan with a Bradley function fit first (black line) (a = 5.44×10^{-9}, b = 693.77, $r^2 = 0.70$) and second iteration (blue line) (a = 5.93×10^{-9}, b = 399.21, $r^2 = 0.97$), The electrophoretic mobilities were measured in duplicates; both duplicates are shown on the graph and included in the fit (see section 3.4.2).

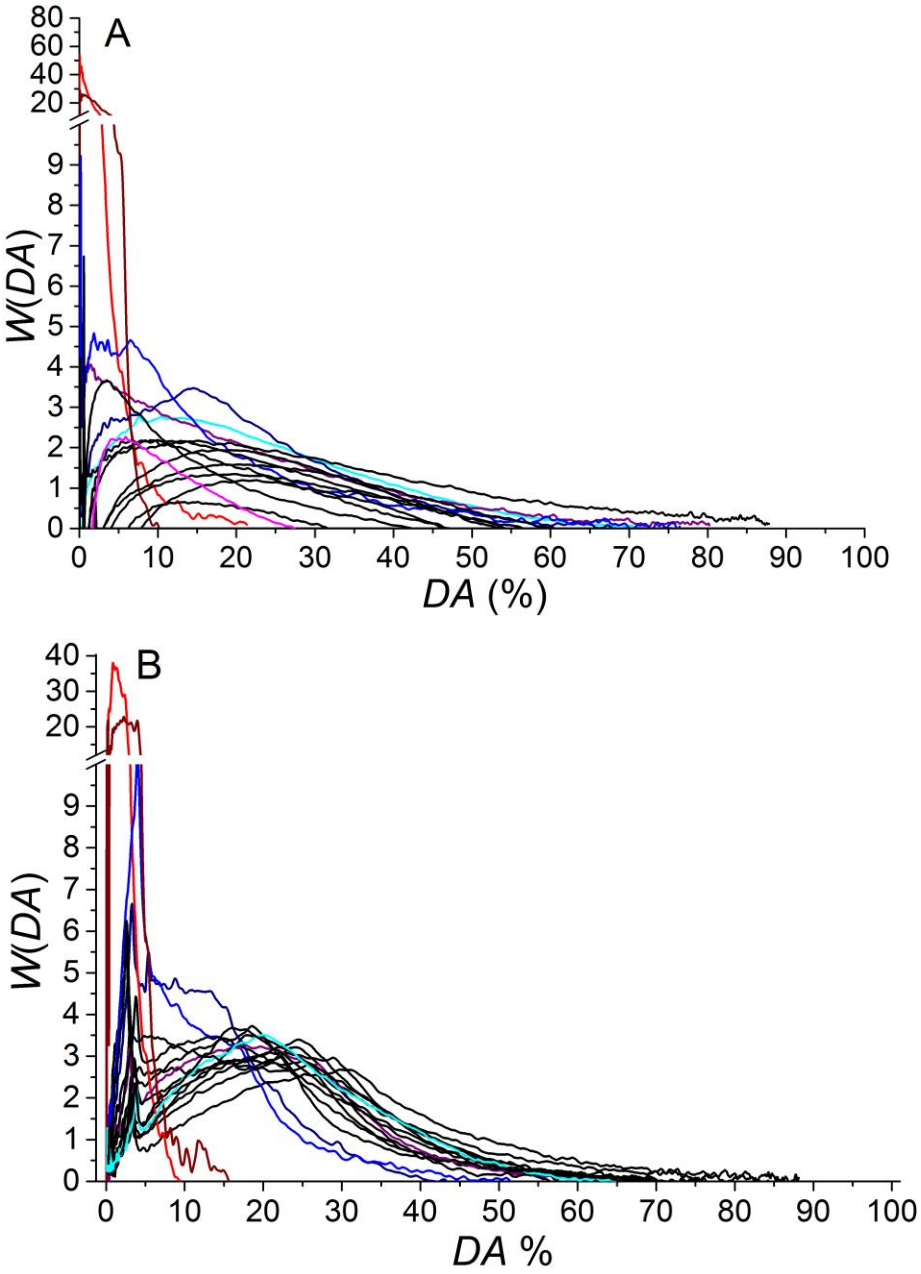

Figure 7. Composition distributions of chitosan samples separated in A. NaPB100 and B. LiPB100

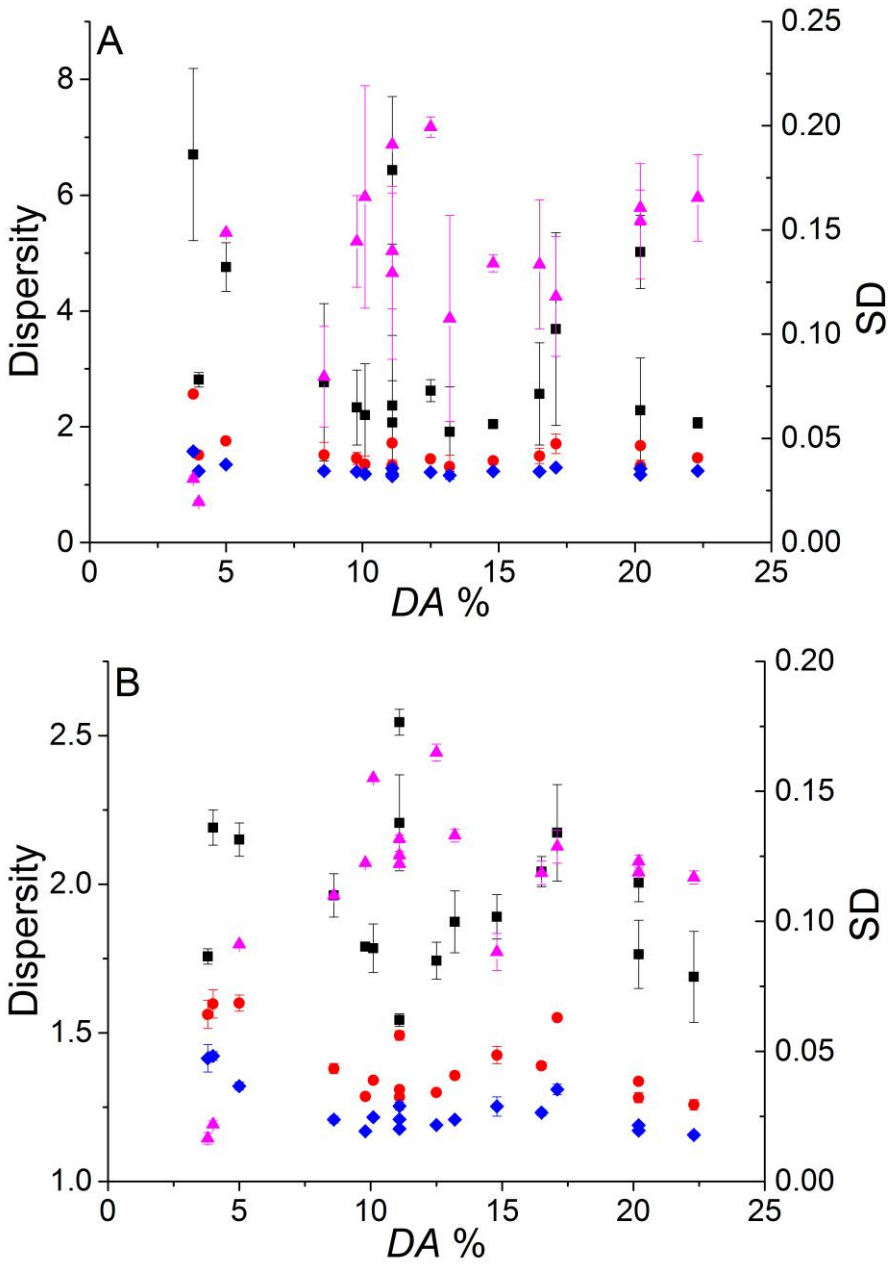

Figure 8. Dispersity of composition distributions as $D(W(DA),1,0)$ (black squares), $D(W(DA),2,0)$ (red circles), $D(W(DA),3,0)$ (blue diamonds) and standard deviation (pink triangles) for chitosan samples separated in A) NaPB100 and B) LiPB100. See supporting information equation S1 to S8 for dispersity calculations [27].

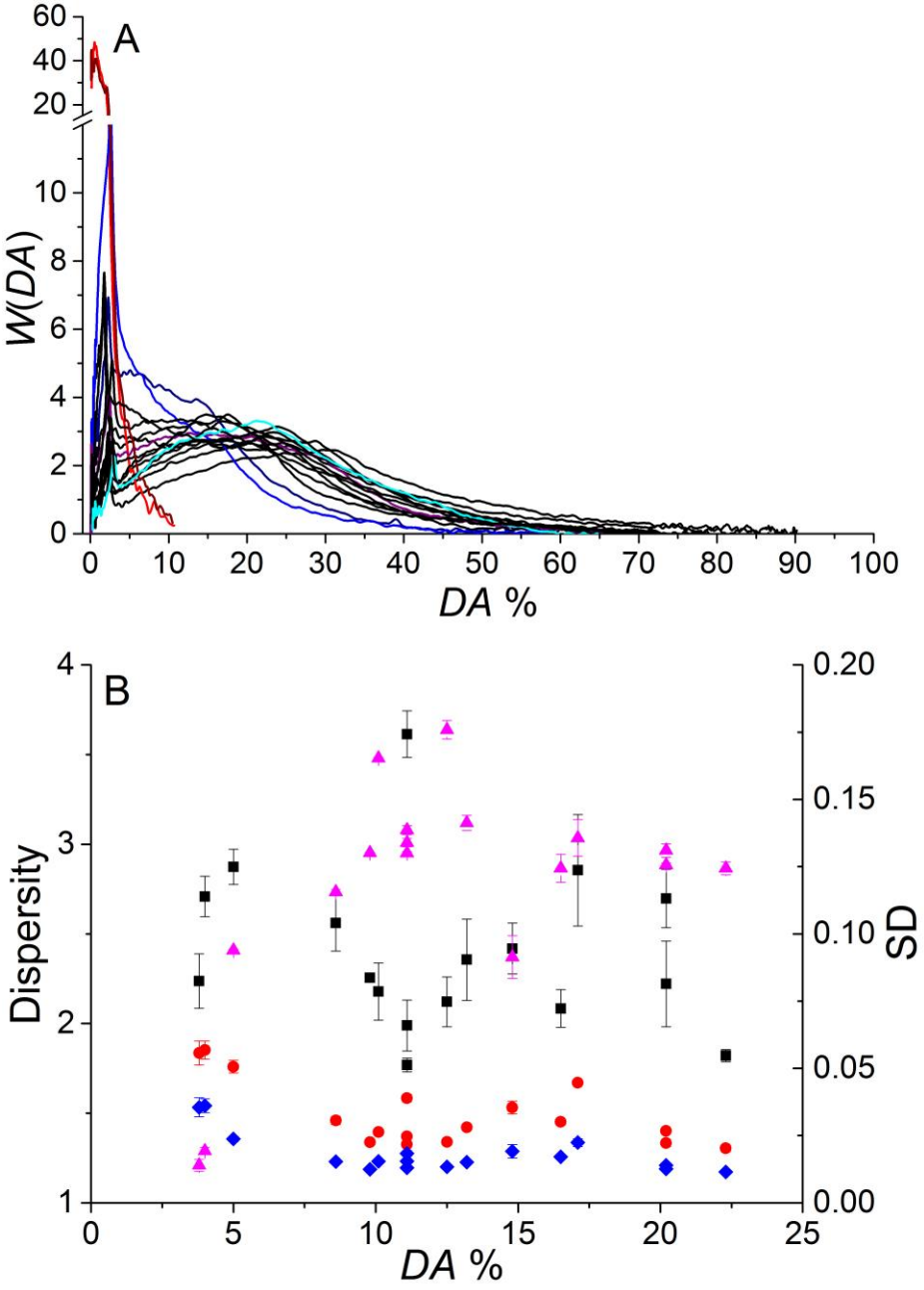

Figure 9. A. Composition distributions and B. Dispersity of composition distributions as *D*(*W*(*DA*),1,0) (black squares), *D*(*W*(*DA*),2,0) (red circles), *D*(*W*(*DA*),3,0) (blue diamonds) and standard deviation (pink triangles) for chitosan samples separated in LiPB100 and treated with the 2nd iteration. See supporting information equation S1 to S8 for dispersity calculations [27].

Supporting Information For

Determination of the Distribution of Degrees of Acetylation of Chitosan

Joel Jerushan Thevarajah[a,b], Matthew Paul Van Leeuwen[a,c], Herve Cottet[d], Patrice Castignolles[b*], Marianne Gaborieau[a,b]

[a] Western Sydney University, Molecular Medicine Research Group (MMRG), Parramatta campus, Locked bag 1797, Penrith 2751, Australia, joel.thevarajah@westernsydney.edu.au, m.gaborieau@westernsydney.edu.au

[b] Western Sydney University, Australian Centre for Research on Separation Sciences (ACROSS), School of Science and Health, Parramatta campus, Locked bag 1797, Penrith 2751, Australia, p.castignolles@westernsydney.edu.au

[c] Western Sydney University, School of Medicine, Parramatta campus, Locked bag 1797, Penrith 2751, Australia, m.vanleeuwen@westernsydney.edu.au

[d] Institut des Biomolécules Max Mousseron (IBMM, UMR 5247 CNRS-Université de Montpellier-Ecole Nationale Supérieure de Chimie de Montpellier), Place Eugène Bataillon CC 1706, 34095 Montpellier Cedex 5, France, herve.cottet@umontpellier.fr

* Corresponding author: p.castignolles@westernsydney.edu.au, tel: +61 2 9685 9970, fax: +61 2 9685 9915

Chitosan samples and supplier information

A number of chitosan samples were analyzed. The samples were commercially available from different suppliers.

Table S1: Information of chitosan samples studied in the manuscript provided by supplier and measured. *DA* is the degree of acetylation in % of monomer units (DA_{supp} was given by the supplier, DA_{SSNMR} was measured by solid-state NMR spectroscopy). The viscosity in cps was given by the supplier in the following conditions: [A] at 20°C; [B] at 1% in 1% AcOH; [C] at 1 % in 1 % AcOH, at 20 °C, according to DIN 45, 100S-1; [D] at 20°C, [B] at 1% in 1% AcOH.

Sample	*Supplier*	*Catalog number*	*Lot*	DA_{supp}	DA_{SSNMR}	*Viscosity*
HighMW1	Sigma-Aldrich	419419	MKBD7240V	22	11.1	1218 [B]
HighMW2	Sigma-Aldrich	419419	12913CJ	24	11.0	1540 [B]
MedMW2	Sigma-Aldrich	448877	03318AJ	20	20.2	590 [B]
MedMW3	Sigma-Aldrich	448877	MKBF1336V	20	13.2	503 [B]
MedMW1	Sigma-Aldrich	448877	MKBH1108V	24	22.3	563 [B]
MedMW4	Sigma-Aldrich	448877	09303PE	25	11.1	453 [B]
LowMW2	Sigma-Aldrich	448869	06714DJ	8.9	5	238 [B]
LowMW1	Sigma-Aldrich	448869	MKBG3334V	3.9	17.1	35 [B]
Sig	Sigma-Aldrich	C3646	120M0028V	12	9.8	
Fluk	Sigma-Aldrich (Fluka)	28191	440698/1	not indicated	8.6	337 [C]
AKbioV1	AK Biotech Ltd		090426V1	13.8	10.1	30 [A]
AKbioV2	AK Biotech Ltd		090423V2	14	16.5	320 [A]
AKbioV3	AK Biotech Ltd		090426V3	14	14.8	570 [A]
AKbioD1	AK Biotech Ltd		090422D1	13.9	12.5	35 [A]
AKbioD2	AK Biotech Ltd		090422D2	9.8	11.1	55 [A]
AKbioD3	AK Biotech Ltd		090422D3	4.4	3.8	55 [A]
chitAL	[1]			2.5	4.0	unknown

Dispersity of the electrophoretic mobility distributions and of the composition distributions (distributions of DAs)

The expressions of dispersity for electrophoretic mobility distributions and composition distributions have recently been established [2]. The expressions are analogous to the calculation of dispersity of molar mass distributions by a ratio of moments. The discrete expressions used to calculate the dispersity are as below:

$$D(W(\mu),1,0) = \frac{[\sum_z W(\mu_z)\mu_z\,(\mu_{z+1}-\mu_z)][\sum_z W(\mu_z)\mu_z{}^{-1}(\mu_{z+1}-\mu_z)]}{[\sum_z W(\mu_z)\,(\mu_{z+1}-\mu_z)]^2} \quad \text{(S1)}$$

$$D(W(\mu),2,0) = \frac{[\sum_z W(\mu_z)\,\mu_z{}^2(\mu_{z+1}-\mu_z)][\sum_z W(\mu_z)\,(\mu_{z+1}-\mu_z)]}{[\sum_z W(\mu_z)\,\mu_z(\mu_{z+1}-\mu_z)]^2} \quad \text{(S2)}$$

$$D(W(\mu),3,0) = \frac{[\sum_z W(\mu_z)\,\mu_z{}^3(\mu_{z+1}-\mu_z)][\sum_z W(\mu_z)\,\mu_z(\mu_{z+1}-\mu_z)]}{[\sum_z W(\mu_z)\,\mu_z{}^2(\mu_{z+1}-\mu_z)]^2} \quad \text{(S3)}$$

$$D(W(DA)1,0) \quad = \frac{[\sum_z W(DA_z)\,DA_z\,(DA_{z+1}-DA_z)][\sum_z W(DA_z)\,DA_z^{-1}\,(DA_{z+1}-DA_z)]}{[\sum_z W(DA_z)\,(DA_{z+1}-DA_z)]^2} \quad \text{(S4)}$$

$$D(W(DA),2,0) = \frac{[\sum_z W(DA_z)\,DA_z{}^2(DA_{z+1}-DA_z)][\sum_z W(DA_z)\,(DA_{z+1}-DA_z)]}{[\sum_z W(DA_z)\,DA_z(DA_{z+1}-DA_z)]^2} \quad \text{(S5)}$$

$$D(W(DA),3,0) = \frac{[\sum_z W(DA_z)\,DA_z{}^3(DA_{z+1}-DA_z)][\sum_z W(DA_z)DA_z\,(DA_{z+1}-DA_z)]}{[\sum_z W(DA_z)\,DA_z{}^2(DA_{z+1}-DA_z)]^2} \quad \text{(S6)}$$

$$D_\sigma = \left[\frac{[\sum_z W(\mu_z)\,(\mu_z-\mu_\mathrm{w})^2(\mu_{z+1}-\mu_z)}{[\sum_z W(\mu_z)\,(\mu_{z+1}-\mu_z)]}\right]^{0.5} \quad \text{(S7)}$$

$$D(W(DA),\sigma,DA_\mathrm{W}) = \left[\frac{[\sum_z W(DA_z)\,(DA_z-DA_\mathrm{w})^2(DA_{z+1}-DA_z)]}{[\sum_z W(DA_z)(DA_{z+1}-DA_z)]}\right]^{0.5} \quad \text{(S8)}$$

Kinetics of chitosan dissolution

Pressure assisted capillary electrophoresis (PACE) measurements of the dissolution of MewMW1 in either 50 mM HCl or 50 mM DCl in D_2O were undertaken with the carousel set to 60 °C.

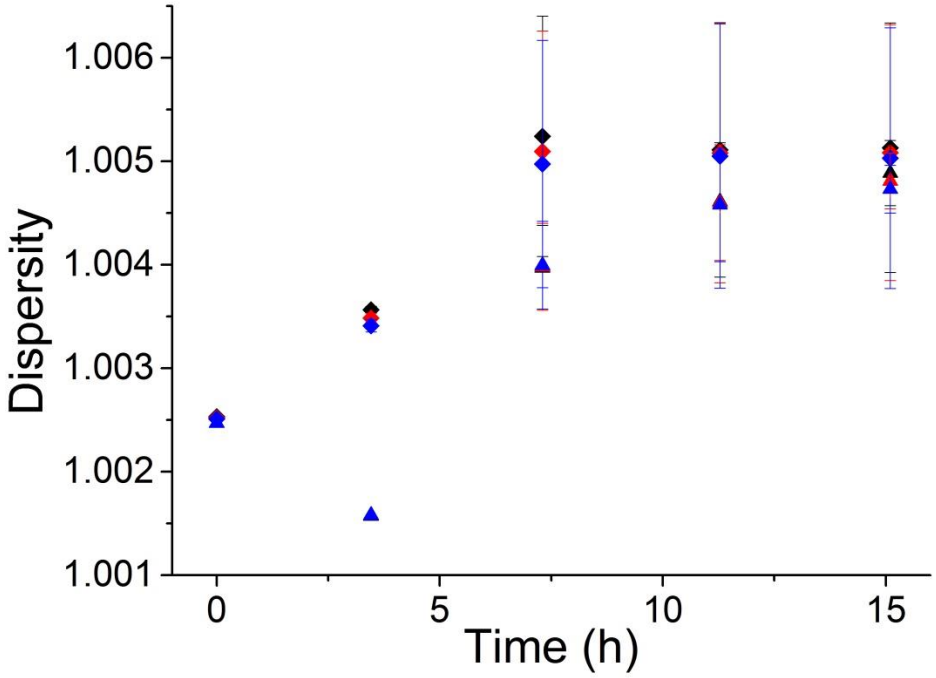

Figure S1: Dispersity of electrophoretic mobility distributions $D(W(\mu),1,0)$ (black), $D(W(\mu),2,0)$ (red), $D(W(\mu),3,0)$ (blue) of chitosan MedMW1 dissolved in 50 mM HCl in H_2O (diamonds) and 50 mM DCl in D_2O (triangles) during kinetic measurement using CE-CC with the carousel kept at 60 °C

Separation of PAlAm

Separation of the cationic polymer poly(allylamine hydrochloride) was possible using a PDADMAC/alginate mulilayer coated capillary. The separation was undertaken using NaPB10 at pH 3. It was detected using both UV absorbance and conductivity.

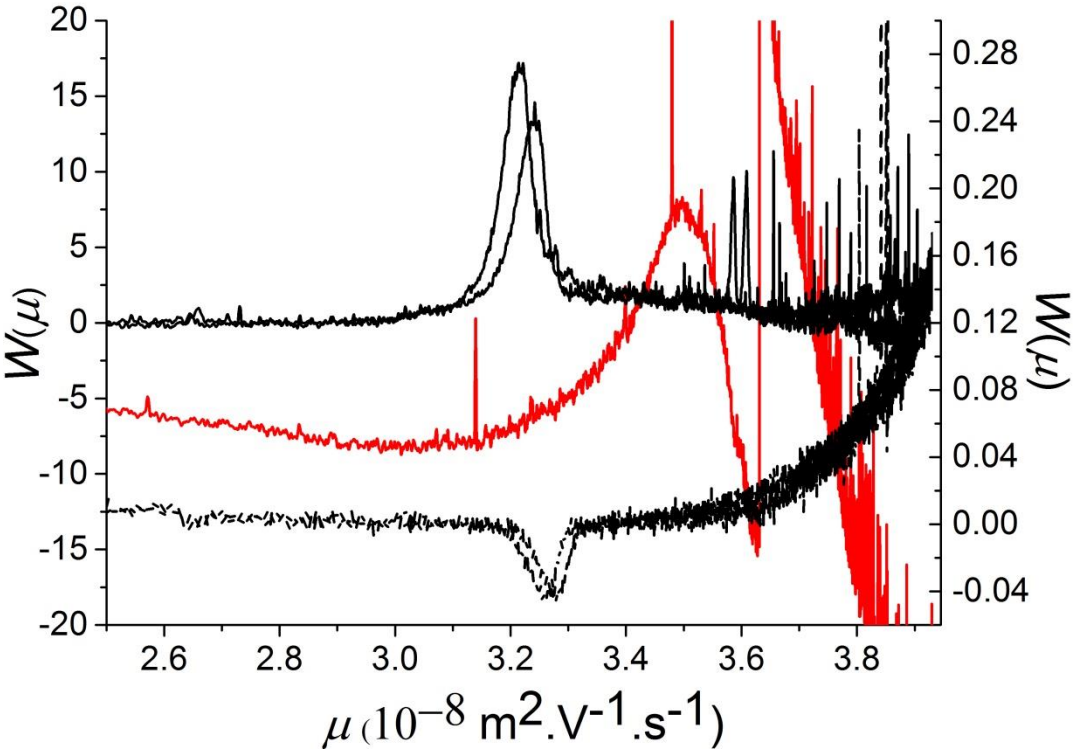

Figure S2: Electropherogram of PAlAm (black lines) and chitosan (red line) separated in a PDADMAC/alginate multilayer coated capillary in NaPB10, detected with UV (solid line – left y axis) or conductivity (dashed line – right y axis).

Correlation of electrophoretic mobility and composition

The weight-average electrophoretic mobility of the complete range of chitosan samples separated in NaPB100 and LiPB100 were plotted against their average *DA* measured by solid-state NMR spectroscopy.

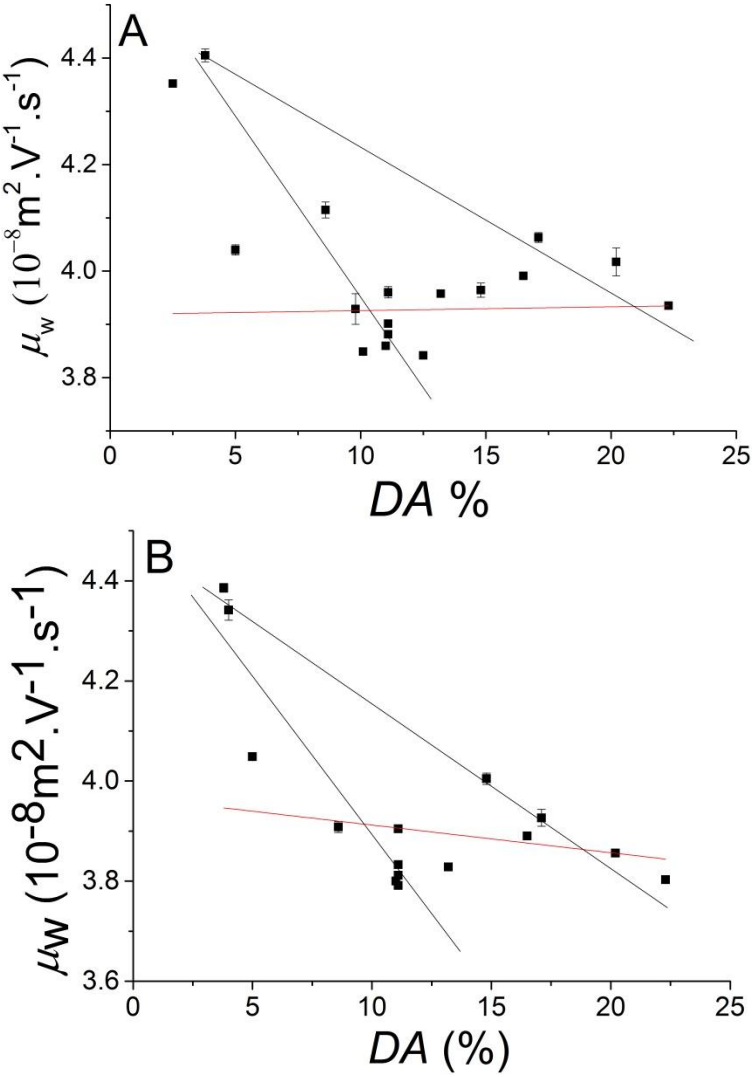

Figure S3 A. Calibration curve of the weight-average electrophoretic mobility (μ_w) of chitosan samples separated in A. NaPB100 and B. LiPB100. Red line represents linear fit and black lines represent possible population fits

Chitosan samples were removed in initial calibration curves based on their dispersity. This was to allow the calibration to curve mimic those made with “narrow” standards. Various fits were tested including linear, polynomial, inverse and log functions.

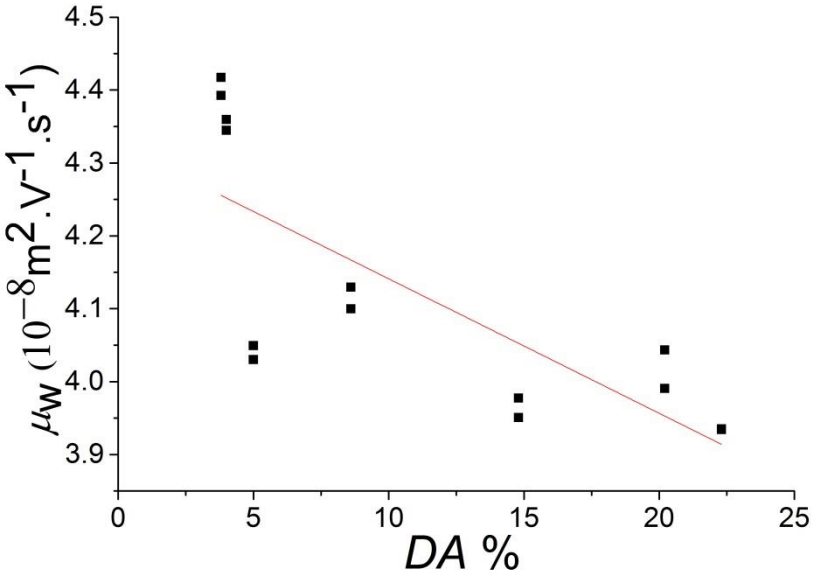

Figure S4: Calibration curve of weight-average electrophoretic mobility in NaPB100 as a function of DA for chitosan with a linear fit (red line) ($r^2 = 0.56$)

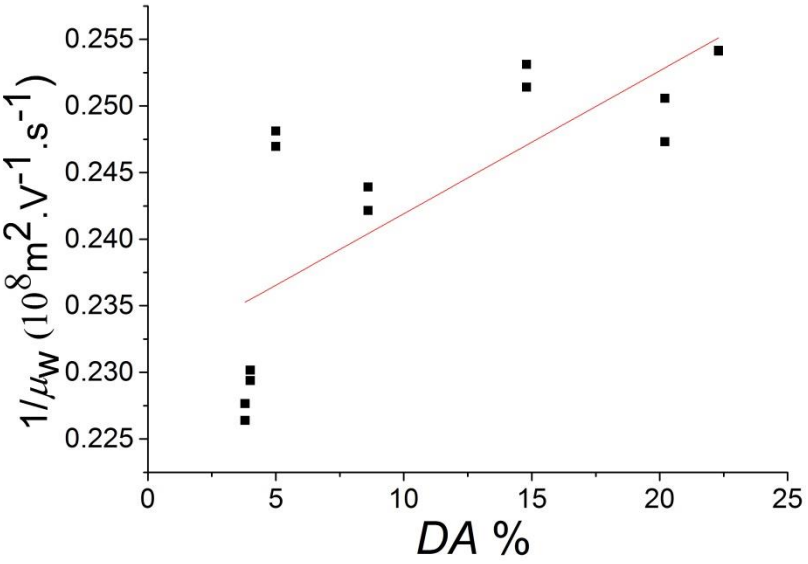

Figure S5: Calibration curve of the inverse function of weight-average electrophoretic mobility in NaPB100 as a function of DA for chitosan with a linear fit (red line) ($r^2 = 0.57$)

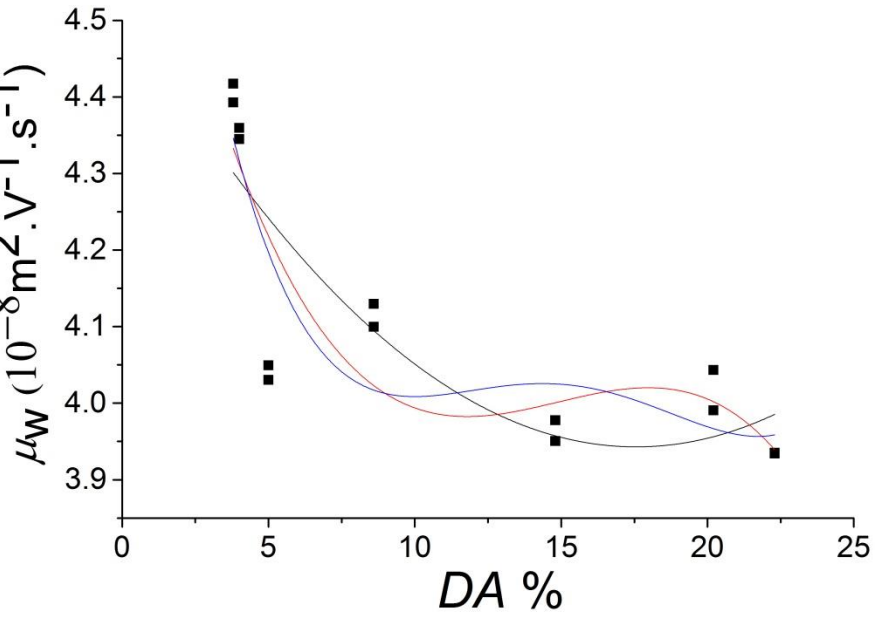

Figure S6: Calibration curve of weight-average electrophoretic mobility in NaPB100 as a function of DA for chitosan with order 2 (black line), 3 (red line) and 4 (blue line) polynomial fit.

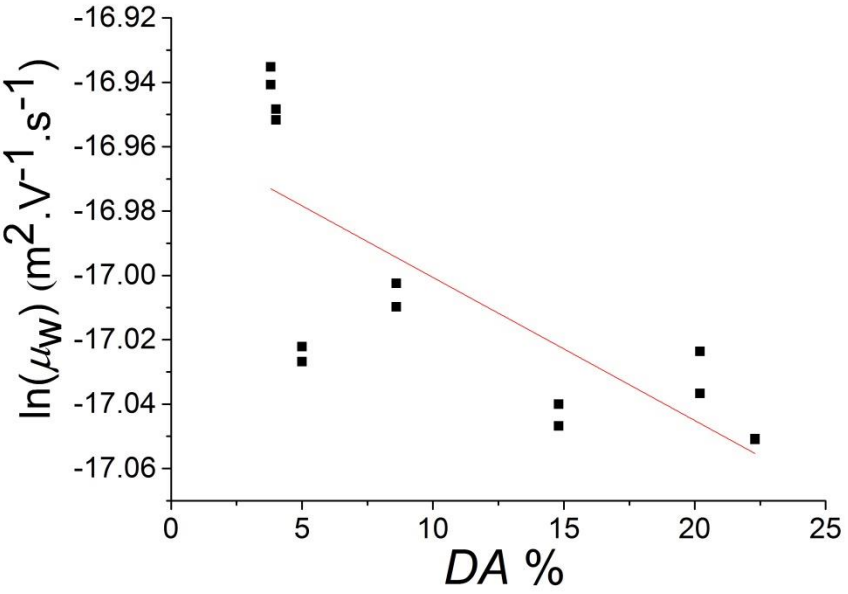

Figure S7: Calibration curve of the log function of weight-average electrophoretic mobility in NaPB100 as a function of DA for chitosan with a linear fit (red line) ($r^2 = 0.56$)

X-ray diffraction of chitosan

Chitosan samples were measured with a Bruker D8 Advance Powder Diffractometer (XRD). Incident radiation was Cu Kα II with detection by a Bruker Lynx eye silicon drift detector. Samples were placed on a sample holder in powder form and levelled to a thin, flat layer.

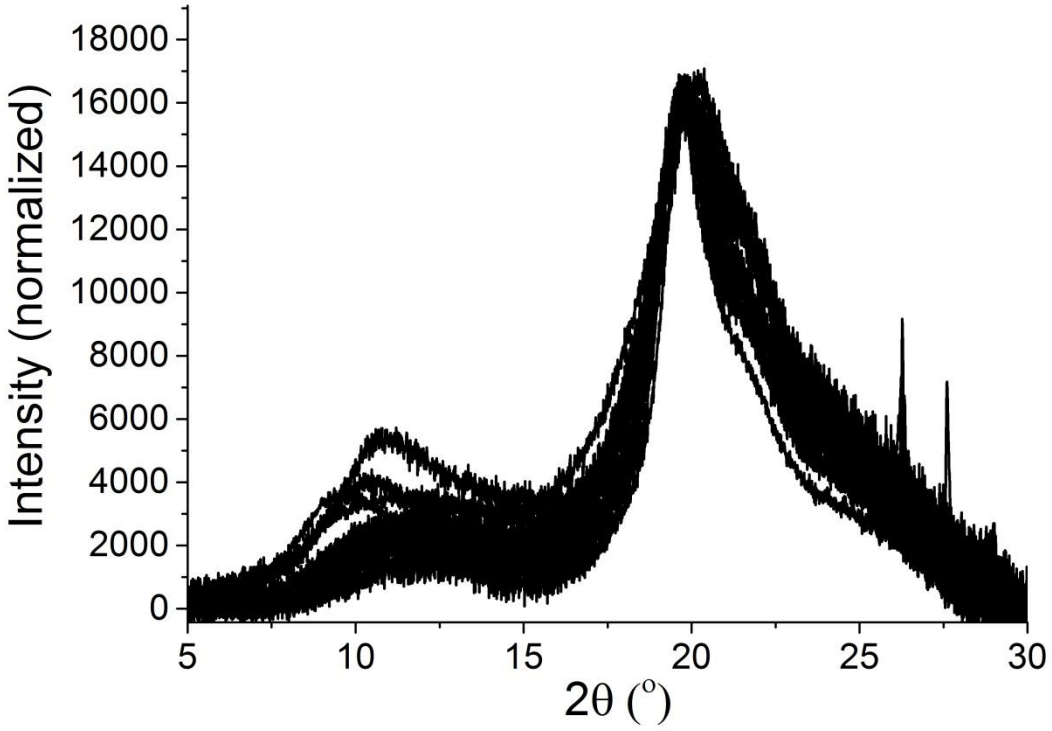

Figure S8: X-ray diffractograms of various chitosan samples normalized by the peak maximum between 18 and 22°.

Composition Distributions

Using the initial composition distributions, the average *DA* at the peak apex could be determined. A second iteration of the calibration was calculated. For chitosan samples separated in NaPB100, the correlation between the *DA* from the peak apex and the weight-average electrophoretic mobility did not improve as seen below. Therefore composition distributions were not calculated.

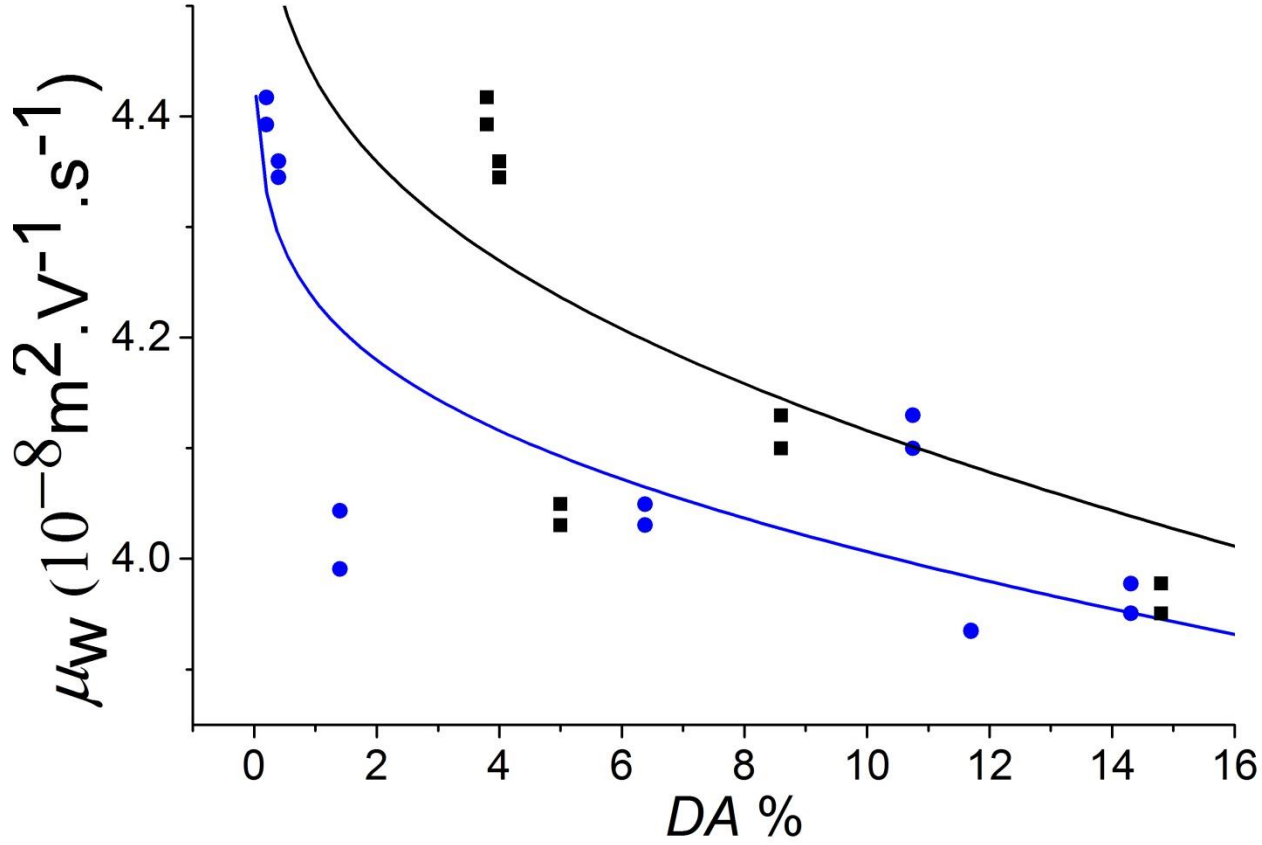

Figure S9: Calibration curve with a Bradley function fit of the weight-average electrophoretic mobility in NaPB100 as a function of *DA* from the solid-state NMR spectroscopy measurements (black) or the peak apex of the composition distributions (blue).

References

[1] M. Mnatsakanyan, J.J. Thevarajah, R.S. Roi, A. Lauto, M. Gaborieau, P. Castignolles, Separation of chitosan by degree of acetylation using simple free solution capillary electrophoresis, Anal. Bioanal. Chem. 405 (2013) 6873-6877.

[2] J.J. Thevarajah, A.T. Sutton, A.R. Maniego, E.G. Whitty, S. Harrisson, H. Cottet, P. Castignolles, M. Gaborieau, Quantifying the Heterogeneity of Chemical Structures in Complex Charged Polymers through the Dispersity of Their Distributions of Electrophoretic Mobilities or of Compositions, Anal. Chem. 88 (2016) 1674-1681.